SIAM J. APPL. MATH.
Vol. 77, No. 3, pp. 854–880

A HYBRID CONTINUOUS/DISCRETE-TIME MODEL FOR INVASION DYNAMICS OF ZEBRA MUSSELS IN RIVERS*

QIHUA HUANG†, HAO WANG‡, AND MARK A. LEWIS§

Abstract. While some species spread upstream in river environments, not all invasive species are successful in spreading upriver. Here the dynamics of unidirectional water flow found in rivers can play a role in determining invasion success. We develop a continuous-discrete hybrid benthic-drift population model to describe the dynamics of invasive freshwater mussels in rivers. In the model, a reaction-advection-diffusion equation coupled to an ordinary differential equation describes the larval dispersal in the drift until settling to the benthos, while two difference equations describe the population growth on the benthos. We study the population persistence criteria based on three related measures: fundamental niche, source-sink distribution, and net reproductive rate. We calculate the critical domain size in a bounded domain by analyzing a next generation operator. We analyze the upstream and downstream spreading speeds in an unbounded domain. The model is parameterized by available data in the literature. Combining the results of model parameterization and theoretical analysis, we numerically analyze how the interaction between population growth and dispersal, river flow rate, and water temperature affects both persistence and the spread of zebra mussels along a river.

Key words. invasion, river, zebra mussel, persistence, critical domain size, spreading speed

AMS subject classifications. 92B05, 45C05, 34K05

DOI. 10.1137/16M1057826

1. Introduction.

The invasion of nonnative species has had pervasive and deleterious impacts on the world's ecosystem [26, 35]. One prominent example is the introduction of the zebra mussel (*Dreissena polymorpha*) into the rivers, lakes, reservoirs, and canals of North America. Because of their high fecundity and strong ability to settle on almost any solid substratum, zebra mussels usually outcompete native bivalves [30], cause large reductions in phytoplankton [2] and zooplankton abundances [6], greatly modify the cycling of nutrients [1], and cause severe damage to waterworks [10]. As a result, zebra mussels not only are "ecosystem engineers" that alter both the structure and function of the environment they invade, but also give rise to significant removal costs to individuals, municipalities, and corporations [34]. It is estimated that zebra mussels cause $1 billion in damages and associated control costs per year [28]. Because of its importance as an invader, there are very good records of the geographic extent and rate of spread of the zebra mussel in various water bodies and countries. Spread in North America has been generally reported at a high level of spatial resolution [3].

*Received by the editors January 22, 2016; accepted for publication (in revised form) February 7, 2017; published electronically May 25, 2017.
http://www.siam.org/journals/siap/77-3/M105782.html
Funding: This work was supported by the NSERC Canadian Aquatic Invasive Species Network. The second author's work was supported by an NSERC Discovery grant. The third author's work was supported by a Canada Research Chair and an NSERC Discovery grant.

†Current address: School of Mathematics and Statistics, Southwest University, Chongqing, 400715, People's Republic of China (qihua@swu.edu.cn). Address when first submitted: Center for Mathematical Biology, Department of Mathematical and Statistical Sciences, University of Alberta, Edmonton, AB, T6G 2G1, Canada.
‡Center for Mathematical Biology, Department of Mathematical and Statistical Sciences, University of Alberta, Edmonton, AB, T6G 2G1, Canada (hao8@ualberta.ca).
§Center for Mathematical Biology, Department of Mathematical and Statistical Sciences, University of Alberta, Edmonton, AB, T6G 2G1, Canada, and Department of Biological Sciences, University of Alberta, Edmonton, AB, T6G 2E9, Canada (mark.lewis@ualberta.ca).

Successful invasion depends upon the size of an invading population at its source as well as the ability of individuals to survive and successfully reproduce at their new destinations. The potential of an aquatic nuisance species to survive and reproduce, once it has been introduced, depends on the levels of physical, chemical, and biological factors (e.g., water temperature, turbidity, flow rates, suitable substrate, calcium concentration, salinity, pH, oxygen, food source) [8, 14, 24]. These environmental factors may vary significantly among different types of water bodies. For instance, in rivers, zebra mussels are most affected by unidirectional water flow, disturbance due to water flow, suspended sediment, and minimal suitable substrates for attachment [14]. Unidirectional water flow makes it difficult for local populations of zebra mussels in rivers to increase in density, as their larvae are swept downstream. However, high densities of zebra mussels can form in the lower courses of rivers because of slow flow and reduced movement of bottom sediments [14]. Since its introduction to North America in 1986, the zebra mussel has invaded several large rivers, including the St. Lawrence, Hudson, Mississippi, Illinois, Ohio, Tennessee, and Arkansas rivers [30].

The main goal of this study is to develop and apply a mathematical model to understand the interaction between population growth and dispersal, environmental conditions, and river flow in determining upstream invasion success of zebra mussels. To this end, we develop a novel, impulsive, spatially explicit model, with distinct dispersal and growth stages, to describe the dynamics of zebra mussels in rivers. In the model, the dynamics of the dispersing larval stage are governed by an advection-diffusion-reaction equation, while juvenile and adult growth is described by two difference equations that map the population density in the current year to the population density in the next year. This couples a population growth model to a physical model for dispersal based on existing understanding of river flow dynamics. The model can be used to investigate how the flow regime and environmental factors influence the distribution, abundance, and spread of zebra mussels in river ecosystems.

To study whether zebra mussels are able to successfully invade a river, we consider persistence criteria for zebra mussels based on our spatially explicit population model. Recently, Krkošek and Lewis [17] proposed three relevant measures of population persistence that relate to lifetime reproductive output in a spatially variable environment. These measures were adapted in [25] to analyze an advection-diffusion-reaction model for a stream population; such a single-compartment model regards the whole river channel as a drift zone and assumes that an unstructured population disperses and reproduces in the drift. In this work, we extend the three measures of population in [25] to our structured continuous-discrete hybrid model.

The first measure of persistence, denoted by $R_{\mathrm{loc}}(x)$, describes the *fundamental niche* of the population. By definition, individuals are assumed to experience only birth and death after being introduced, but dispersal is excluded. In this work, we use $R_{\mathrm{loc}}(x)$ to answer the following question: If an individual adult is introduced at location x, in the absence of larval dispersal, how many adult offspring will it produce (after undergoing reproduction, larval settlement, and the growth of settled larvae and juveniles) over its lifetime? Thus, in the absence of dispersal, a population will persist at the location x if $R_{\mathrm{loc}}(x) > 1$, it but will not persist if $R_{\mathrm{loc}}(x) < 1$.

The second measure of persistence, denoted by $R_\delta(x)$, describes the *source-sink distribution*. It represents lifetime contributions of an individual introduced at x, undergoing reproduction, dispersal, and survival. In this work, we use $R_\delta(x)$ to answer the following question: If an individual adult is introduced at location x and undergoes reproduction, larval dispersal and settlement, and the growth of settled larvae and juveniles, how many adult offspring will be contributed by the originally

introduced adult over its lifetime? Locations where $R_\delta(x) > 1$ function as sources because each adult at location x on average produces more than one adult in the whole spatial domain over its lifetime. Locations where $R_\delta(x) < 1$ function as sinks because on average the lifetime reproductive output of an adult, introduced at location x, is less than one. Although $R_\delta(x)$ maps how source and sink distribution changes in the spatial habitat, it does not inform about the global persistence or extirpation of a population. To do so we need the final measure of persistence, the *net reproductive rate*, R_0.

Mathematically, R_0 is defined as the spectral radius of the next generation operator. Biologically, in this work, it can be interpreted as the average number of adults produced by a single adult over its lifetime, assuming that the adult is subject to a particular spatial configuration in the river. More precisely, this spatial configuration is an asymptotically stable next generation distribution associated with R_0. As a threshold parameter, R_0 is a powerful measure for studying population persistence in demography and ecology. The population will grow if $R_0 > 1$, but the population will become extirpated if $R_0 < 1$.

We then study the population persistence through critical domain size, which is the minimum length of suitable river habitat required for a population to persist in a river. It results from the assumption that a population can grow locally within a bounded habitat, but might be lost from the habitat to an uninhabitable exterior by movement across the boundary. We calculate the critical domain sizes under two different types of boundary conditions by analyzing the next generation operator, which is introduced to define R_0.

While some species spread upstream in river environments, not all invasive species are successful in spreading upriver. Here the dynamics of unidirectional water flow found in rivers can play a role in determining invasion success. Based on our spatial model, we calculate spreading speeds for a population in a river, both downstream (in the direction of advection) and upstream. By doing so, we are able to understand the interaction between population growth and dispersal and river flow in determining upstream invasion success.

The model is parameterized based on experimental data on zebra mussel populations found in the literature. In particular, the survival and the growth in body size are based on measured functions of temperature, and the dispersal is given by the river flow dynamics. We then apply the results of model parameterization to numerically calculate three measures of population persistence, critical domain size, and propagation speeds for zebra mussels in a river. The numerical results illustrate how water temperature and river flow dynamics affect the persistence and propagation of zebra mussels in a river.

The rest of the paper is organized as follows. In section 2, we develop a spatially explicit population model that describes the growth and dispersal of the zebra mussel along a river. In section 3, we introduce three measures of population persistence. In section 4, we calculate the critical domain size by analyzing the next generation operator. In section 5, we calculate the downstream and upstream spreading speeds. In section 6, we connect model to data via model parameterization. In section 7, the numerical results are presented to illustrate the influence of temperature and river flow on population persistence. Finally a brief discussion section completes the paper.

2. Model formulation. In this section, we develop a spatially explicit model for the growth and spread of the zebra mussel (*Dreissena polymorpha*) in a river, based on the life cycle of the zebra mussel. There are three main periods in the zebra

mussel life cycle: the larval, juvenile, and adult stages. The larvae are planktonic, drifting in a water column and eventually settling on a substrate. The juvenile state begins after the settlement and ends when mussels become sexually mature. Mussels are considered adults when they become sexually mature. On average, zebra mussels live 2–5 years and can reproduce in their second year. Adult zebra mussels start to reproduce when the water they live in is warm enough, usually starting in spring or summer. The larval life stage is relatively short (from a few days to a few weeks [32]) compared to the zebra mussel lifespan (a few years). As a result, a model for the spread of zebra mussels in a river requires the introduction of different time scales.

To describe the dynamics of a zebra mussel population in a river, we define $u(x,t)$ and $w(x,t)$ as the density of dispersing larvae in the drift (number per volume) and the density of settled larvae on the benthos (number per area), respectively, at location x and time t. We assume that the larvae disperse, settle, and die continuously for time $t \in [0,\tau]$. We let $J(x,n)$ and $A(x,n)$ denote the density of juveniles (number per area) and the density of adults (number per area), respectively, at the beginning of the breeding season in year n ($n = 0,1,2,\ldots$). The mathematical model that describes the spatial dynamics of the population undergoing growth and dispersal in a river of length L is given by

(2.1)
$$
\begin{aligned}
&u_t = \tfrac{1}{q(x)}(D(x)q(x)u_x)_x - \tfrac{Q}{q(x)}u_x - m(x)u - \sigma(x)u, \quad x \in (0,L), \quad t \in (0,\tau),\\
&w_t = h(x)\sigma(x)u, \quad x \in (0,L), \quad t \in (0,\tau),\\
&J(x,n+1) = \varphi(x,n)s_l(x,T)w(x,\tau), \quad x \in (0,L),\\
&A(x,n+1) = \varphi(x,n)[s_j(x,T)J(x,n) + s_a(x,T)A(x,n)], \quad x \in (0,L),\\
&\alpha_1 u(0,t) - \alpha_2 u_x(0,t) = 0, \quad \alpha_3 u(L,t) + \alpha_4 u_x(L,t) = 0, \quad t \in (0,\tau),\\
&u(x,0) = r(x)A(x,n)/h(x), \quad w(x,0) = 0, \quad x \in (0,L),\\
&J(x,0) = J^0(x), \quad A(x,0) = A^0(x), \quad x \in (0,L).
\end{aligned}
$$

In this model, the first equation presents a generic description of the random movement, downstream advection, mortality, and settlement of larvae in the water column. Here, $q, D \in C^2([0,L],(0,\infty))$ are the cross-sectional area of the river and the spatially variable diffusion coefficient, respectively, $Q > 0$ is the constant discharge, and $m(x) > 0$ and $\sigma(x) > 0$ are the spatially varying larval mortality rate and settling rate, respectively. We assume that there exist positive constants $\underline{m}$ and $\underline{\sigma}$ such that $m(x) > \underline{m}$ and $\sigma(x) > \underline{\sigma}$ for all $x \in [0,L]$. See [21] for the derivation of the first equation of (2.1) from a three-dimensional conservation law for movement of individuals in streams. The second equation of (2.1) describes the rate of change of the density of settled larvae on the benthos. Here, $h(x)$ is the spatially variable water depth which rescales the population densities. For the benthic density w is defined as number of larvae divided by benthic area, while the drifting density u is defined as number of larvae divided by water volume (which can be calculated by the benthic area multiplied by the water depth h). We assume that there exists a positive constant $\bar{h}$ such that $h(x) < \bar{h}$ for all $x \in [0,L]$.

The third and fourth equations of (2.1) describe the population growth on the benthos from year to year. Here, $s_l(x,T)$, $s_j(x,T)$, and $s_a(x,T)$ are the basal survival rates for larvae, juveniles, and adults, respectively, and they are functions of location x and water temperature T. The function $\varphi(x,n)$ accounts for the density-dependent survival of the population due to competition for limiting resources such as nutrients or

space. Following [17], we choose a modified Beverton–Holt density-dependent survival term:

$$\varphi(x,n) = \frac{1}{1+\beta[\ell_l(T)w(x,\tau)+\ell_j(T)J(x,n)+\ell_a(T)A(x,n)]}, \tag{2.2}$$

where β is the competition coefficient that relates competitive ability to a phenotypic trait, and $\ell_l(T)$, $\ell_j(T)$, and $\ell_a(T)$ are taken as the shell lengths of larvae, juveniles, and adults, respectively. We assume that $\ell_l(T)$, $\ell_j(T)$, and $\ell_a(T)$ are functions of temperature T. We also assume that β is the same for each life-history stage and that variation in competitive ability among stages is accounted for in $\ell_l(T)$, $\ell_j(T)$, and $\ell_a(T)$. By assuming that individuals compete for a limiting source (food), Huang et al. [9] derived a nonspatial analogue of (2.2). A derivation of the survival term (2.2) is provided in section S1 in the supplemental material (M105782SupMat.pdf [local/web 265KB]).

The equation $u(x,0) = r(x)A(x,n)/h(x)$ represents the density of larvae reproduced by adults during breeding season. Here $1/h(x)$ translates the population density per unit benthic area into the population density per unit river volume. The initial density of settled larvae $w(x,0)$ is assumed to be zero. $J^0(x)$ and $A^0(x)$ are the initial distributions of juveniles and adults, respectively.

The boundary conditions corresponding to the first equation are either Dirichlet ($\alpha_1 = \alpha_3 = 1$, $\alpha_2 = \alpha_4 = 0$), Neumann ($\alpha_1 = \alpha_3 = 0$, $\alpha_2 = \alpha_4 = 1$), or Robin ($\alpha_i \geq 0$, $\alpha_1 + \alpha_3 \neq 0$, $\alpha_2 + \alpha_4 \neq 0$) conditions. In particular, we allow for two types of boundary conditions relevant to rivers, which are referred to as *hostile* and *Danckwerts'* boundary conditions in [25]. Hostile conditions represent zero-flux at the river source (no individuals leave or enter the domain at the upstream boundary) and zero-density at the river outflow (all individuals die at the downstream boundary):

$$Qu(0,t) - D(0)q(0)u_x(0,t) = 0 \quad \text{and} \quad u(L,t) = 0. \tag{2.3}$$

Danckwerts' conditions also assume zero-flux at the upstream boundary but use a free-flow or insulated condition at the downstream boundary (e.g., the river discharges all individuals into a region such as a lake or a waterfall, from which they cannot return [31]):

$$Qu(0,t) - D(0)q(0)u_x(0,t) = 0 \quad \text{and} \quad u_x(L,t) = 0. \tag{2.4}$$

See [21] for a derivation and discussion of these boundary conditions from a random-walk perspective. For convenience, we define the strongly elliptic linear operator

$$\mathcal{L} := \frac{1}{q(x)}\frac{\partial}{\partial x}\left(D(x)q(x)\frac{\partial}{\partial x}\right) - \frac{Q}{q(x)}\frac{\partial}{\partial x},$$

which represents both the random dispersal due to turbulence and intrinsic movement of individuals and the directed dispersal due to downstream flow, respectively. The first equation in (2.1) can then be written as

$$u_t = \mathcal{L}u - m(x)u - \sigma(x)u.$$

The model (2.1) is an extension of the impulsive reaction-diffusion model studied in [18]. Based on the impulsive model, Lewis and Li [18] developed a spatially explicit theoretical framework that links a population's vital rates and dispersal characteristics with its spreading speeds and traveling waves speeds, as well as minimal domain size for population persistence.

3. Three measures of population persistence. In this section, we define three measures of population persistence, described in the introduction, in a spatially variable environment. Note that $(w^*, J^*, A^*) \equiv (0, 0, 0)$ is the trivial solution of the system consisting of the third and fourth equations of (2.1); we consider the associated linearized system of (2.1) at (w^*, J^*, A^*) in this section. For simplicity, we set $s_l(x, T) := s_l(x)$, $s_j(x, T) := s_j(x)$, and $s_a(x, T) := s_a(x)$.

3.1. Fundamental niche, $R_{\mathrm{loc}}(x)$. The first measure of persistence, denoted by $R_{\mathrm{loc}}(x)$, determines fundamental niche space. By definition, it strictly excludes dispersal and competition. In this scenario, model (2.1) reduces to

$$
\begin{aligned}
&u_t = -m(x)u - \sigma(x)u, \quad x \in (0, L),\ t \in (0, \tau),\\
&w_t = h(x)\sigma(x)u, \quad x \in (0, L),\ t \in (0, \tau),\\
&J(x, n+1) = s_l(x)w(x, \tau), \quad x \in (0, L),\\
&A(x, n+1) = s_j(x)J(x, n) + s_a(x)A(x, n), \quad x \in (0, L),\\
&u(x, 0) = r(x)A(x, n)/h(x), \quad w(x, 0) = 0, \quad x \in (0, L),\\
&J(x, 0) = J^0(x), \quad A(x, 0) = A^0(x), \quad x \in (0, L).
\end{aligned} \tag{3.1}
$$

Solving the first equation of (3.1), we obtain

$$
u(x, t) = \frac{r(x)A(x, n)}{h(x)} e^{-(m(x)+\sigma(x))t}. \tag{3.2}
$$

Integrating the second equation of (3.1) on $[0, \tau]$ and using (3.2) yields

$$
w(x, \tau) = \frac{\sigma(x)r(x)[1 - e^{-(m(x)+\sigma(x))\tau}]}{m(x) + \sigma(x)} A(x, n) := \Theta(x)A(x, n). \tag{3.3}
$$

This means that the number of settled larvae produced by an adult at location x is $\Theta(x)$. These settled larvae may survive until they grow into juveniles and adults at the rate of $s_l(x)$ and $s_j(x)$, respectively. Thus, in the absence of larval dispersal, the number of adult offspring produced by an initially introduced adult at location x in the first year is given by $\Theta(x)s_l(x)s_j(x)$. Moreover, the probability that such an initially introduced adult will survive until the next year is $s_a(x)$; hence it will yield $s_a(x)\Theta(x)s_l(x)s_j(x)$ adult offspring in the second year. Similarly, in the third year, the number of adult offspring produced by the initial adult is given by $(s_a(x))^2\Theta(x)s_l(x)s_j(x)$.

We define $R_{\mathrm{loc}}(x)$ to be the number of adult offspring produced by an adult, initially introduced at location x, over its lifetime. That is,

$$
\begin{aligned}
R_{\mathrm{loc}}(x) &= \Theta(x)s_l(x)s_j(x) + s_a(x)\Theta(x)s_l(x)s_j(x) + (s_a(x))^2\Theta(x)s_l(x)s_j(x) + \cdots\\
&= \frac{s_l(x)s_j(x)\Theta(x)}{1 - s_a(x)} = \frac{r(x)s_l(x)s_j(x)\sigma(x)[1 - e^{-(m(x)+\sigma(x))\tau}]}{[1 - s_a(x)][m(x) + \sigma(x)]}.
\end{aligned} \tag{3.4}
$$

It follows from the definition of $R_{\mathrm{loc}}(x)$ that if $R_{\mathrm{loc}}(x) > 1$, an adult introduced at location x will yield more than one adult at x in the next generation, and the population at x will increase over the generations. Therefore, locations with $R_{\mathrm{loc}}(x) > 1$ correspond to the fundamental niches of the species.

It is worth mentioning that $R_{\mathrm{loc}}(x)$ can be defined in an alternative way as follows. Substituting (3.3) into the third equation of (3.1), we can rewrite the third and fourth equations of (3.1) into the following matrix form:

$$\begin{pmatrix} J(x,n+1) \\ A(x,n+1) \end{pmatrix} = \mathbf{P}(x) \begin{pmatrix} J(x,n) \\ A(x,n) \end{pmatrix}, \tag{3.5}$$

where

$$\mathbf{P}(x) = \begin{pmatrix} 0 & s_l(x)\Theta(x) \\ s_j(x) & s_a(x) \end{pmatrix}$$

is called the projection matrix. We decompose $\mathbf{P}$ into transition and fecundity components, $\mathbf{P} = \mathbf{T} + \mathbf{F}$, where

$$\mathbf{T}(x) = \begin{pmatrix} 0 & 0 \\ s_j(x) & s_a(x) \end{pmatrix}, \qquad \mathbf{F}(x) = \begin{pmatrix} 0 & s_l(x)\Theta(x) \\ 0 & 0 \end{pmatrix}. \tag{3.6}$$

This decomposition allows for the calculation of the net reproductive rate, $R_0(x)$, defined mathematically as

$$R_0(x) = \rho[\mathbf{F}(x)(\mathbf{I} - \mathbf{T}(x))^{-1}], \tag{3.7}$$

where $\mathbf{I}$ is the identity matrix and $\rho[\cdot]$ denotes the spectral radius of the matrix $\mathbf{F}(\mathbf{I}-\mathbf{T})^{-1}$, which is referred to as the next generation matrix [19]. It has been shown [5] that when $R_0(x) > 1$, the population grows, and when $R_0(x) < 1$, the extinction state is stable.

From (3.6) and (3.7), we obtain

$$R_0(x) = \frac{\Theta(x)s_l(x)s_j(x)}{1 - s_a(x)} = \frac{r(x)s_l(x)s_j(x)\sigma(x)[1 - e^{-(m(x)+\sigma(x))\tau}]}{[1 - s_a(x)][m(x) + \sigma(x)]},$$

which is equivalent to (3.4). Hence, the fundamental niche $R_{\mathrm{loc}}(x)$ can be thought of as a spatial extension of the net reproductive rate for nonspatial matrix population models.

3.2. Source-sink distribution, $R_\delta(x)$. To define $R_\delta(x)$ we need to analyze how larval dispersal and settling behaviors contribute to population spread in the river. These behaviors are governed by the first two differential equations of (2.1). To describe the effect of larval dispersal on source-sink dynamics, we first introduce a dispersal kernel, $k(x,y)$, which represents the probability density that a larva reproduced at location y will settle at location x. This kernel satisfies $\int_0^L k(x,y)dx \le 1$. To simplify our analysis we assume that the length of the settlement interval, τ, is sufficiently large for all settlement to effectively occur over the settlement interval ($\tau \gg 1/[\min_{x\in[0,L]}\{m(x) + \sigma(x)\}]$). Based on the first two differential equations of (2.1), we are able to show that $k(x,y)$ is an approximation of the solution of a boundary value problem of an ordinary differential equation.

THEOREM 3.1. *For a fixed value of $y \in [0,L]$, the probability density that a larva reproduced at location y will settle at location x is given by $k(x,y) = h(x)\sigma(x)[\hat{k}(x,y)+\epsilon(x,y)]$, where $\hat{k}(x,y)$ is the solution of the following ordinary boundary value problem:*

$$\begin{aligned} &\mathcal{L}\hat{k}(x,y) - [m(x) + \sigma(x)]\hat{k}(x,y) = -\delta(x-y)/h(x), \quad x \in (0,L), \\ &\alpha_1\hat{k}(0,y) - \alpha_2\hat{k}'(0,y) = 0, \\ &\alpha_3\hat{k}(L,y) + \alpha_4\hat{k}'(L,y) = 0, \end{aligned} \tag{3.8}$$

where $'$ denotes differentiation with respect to x. For a finite τ, $\epsilon(x,y)$ is bounded uniformly in space by $[\exp(-\tau \min_{x\in[0,L]}\{m(x)+\sigma(x)\})] \cdot [\max_{x\in[0,L]}\{h(x)\}]$. *The error term $\epsilon \to 0$ as $\tau \to \infty$.*

The proof of Theorem 3.1 is provided in Appendix A. Actually, ϵ is extremely small for realistic parameter values. This is shown in section 6, where it is approximately e^{-43}.

The solution to (3.8) is a Green's function (see Chapter 7 in [7] and Chapter 3 in [33]). In particular, when q, D, m, σ, and h are constant, by arguments similar to those in [25], we are able to obtain an explicit expression for the Green's function $\hat{k}(x,y)$ (Appendix B).

With the introduction of the dispersal kernel, we are ready to define the second measure of population persistence, denoted by $R_\delta(x)$. The function $R_\delta(x)$ describes the contributions to adult offspring from an adult introduced at location x over its lifetime, undergoing reproduction, larval dispersal, and growth dynamics. Thus, $R_\delta(x)$ must account for the larval dispersal and subsequential survival of offspring to adulthood through a spatially continuous river. According to the definition of dispersal kernel, the total number of settled larvae produced by a single adult at x is given by $r(x)\int_0^L k(y,x)dy$. For a low-density population ($\varphi(x,n) \approx 1$), the probability that a larva settling at location $y \in [0,L]$ will survive to reach the adult stage is $s_l(y)s_j(y)$. Thus, the number of adult offspring produced in the first year is $r(x)\int_0^L k(y,x)s_l(y)s_j(y)dy$. Moreover, the probability that the initially introduced adult will survive until the next year is $s_a(x)$; hence the number of adult offspring yielded in the second year is $s_a(x)r(x)\int_0^L k(y,x)s_l(y)s_j(y)dy$. Similarly, the number of adult offspring yielded in the third year is $(s_a(x))^2 s_l(y)s_j(y)r(x)\int_0^L k(y,x)dy$. Therefore, the total number of adult offspring yielded by a single adult at location x over its lifetime $R_\delta(x)$ can be defined as

$$
\begin{aligned}
R_\delta(x) &= [1 + s_a(x) + (s_a(x))^2 + \cdots]r(x)\int_0^L s_l(y)s_j(y)k(y,x)dy \\
&= \frac{r(x)}{1-s_a(x)}\int_0^L s_l(y)s_j(y)k(y,x)dy.
\end{aligned} \tag{3.9}
$$

Locations where $R_\delta(x) > 1$ act as sources, because a single adult introduced at location x will produce more than one adult offspring in the whole river domain $[0,L]$ over its lifetime. Locations where $R_\delta(x) < 1$ serve as sinks, because the lifetime reproductive output of an adult introduced at location x will result in less than one adult offspring in the whole river. Thus, $R_\delta(x)$ is a measure of the source-sink dynamics in the river.

3.3. Net reproductive rate, R_0. Equation (3.9) maps how lifetime contributions from an individual change with locations in a river. However, it does not provide information on the global persistence or extirpation of the species. To do this we need to introduce a next generation operator, denoted by Γ, in the context of arbitrary initial population distribution.

The definition of our next generation operator is based on the following mathematical setting. In the case where both upstream and downstream boundary value conditions are Neumann or Robin boundary conditions (e.g., Danckwerts' boundary conditions), let $X = C([0,L],\mathbb{R})$ denote the Banach space of continuous functions on the interval $[0,L]$ with the supremum norm $\|f\|_\infty = \max_{x\in[0,L]}|f(x)|$ for $f \in X$. The

set of nonnegative functions forms a solid cone X_+ in the Banach space X. In the case where one or two boundary conditions are Dirichlet boundary conditions (e.g., hostile boundary conditions), let $U = C_0([0, L], \mathbb{R})$ denote the Banach space of continuous functions on $[0, L]$ vanishing on the boundary with the cone U_+ of nonnegative functions in U. Let $U_1 = C^1([0, L], \mathbb{R})$ be the Banach space of continuously differentiable functions on $[0, L]$ with the norm $||f||_1 = \max_{x\in[0,L]} |f(x)| + \max_{x\in[0,L]} |f'(x)|$. Let X be the closed subspace of U_1 consisting of continuously differentiable functions vanishing on the boundary. The set $X_+ = X \cap U_+$ is a solid cone in X.

For any small initial adult distribution $A(x)$ of the spatial model (2.1), the associated next generation adults will be distributed according to

$$(\Gamma A)(x) = s_l(x)s_j(x) \int_0^L \frac{r(y)}{1 - s_a(y)} A(y)k(x, y)dy, \quad x \in [0, L], \tag{3.10}$$

where the integral term sums the contributions from all locations y towards the settled larvae at location x. The term $s_l(x)s_j(x)$ represents the probability that a settled larva grows into an adult. Define

$$R_0 := \rho(\Gamma), \tag{3.11}$$

where $\rho(\Gamma)$ is the spectral radius of the linear operator Γ on X. We call R_0 the *net reproductive rate*, which represents the average number of offspring an individual may produce during its lifetime.

Similar to the next generation operator in [25] (see equation (2.13) therein), we can show that the operator defined by (3.10) is a bounded, compact, linear operator on X (see Proposition 2.6 in [25]). Then the Krein–Rutman theorem implies that R_0 is the dominant eigenvalue of the next generation operator Γ with a positive eigenfunction. That is, there exists a positive function $\phi(x)$ such that

$$\Gamma\phi(x) = R_0\phi(x).$$

We refer to ϕ as the *dominant eigenfunction* associated with R_0.

Although R_0 cannot be thought of conceptually in terms of defining the fundamental niche $R_{\text{loc}}(x)$ or source-sink regions $R_\delta(x)$, it does provide a global measure of population persistence for the spatial model (over all initial conditions); that is, after introduction, the population will grow at an intergenerational rate R_0, and the spatial distribution of the adults will stabilize at $\phi(x)$.

In this paper, we say that a population described by (2.1) will invade and persist in the river if there exists $\varepsilon > 0$ such that for any $A(x, 0) = A_0(x) \in X_+\backslash\{0\}$ we have

$$\liminf_{n\to\infty} \min_{x\in[0,L]} A(x, n) \geq \varepsilon \tag{3.12}$$

when the boundary conditions in (2.1) are Neumann or Robin conditions and

$$\liminf_{n\to\infty} \max_{x\in[0,L]} A(x, n) \geq \varepsilon \tag{3.13}$$

when at least one of the boundary conditions is a Dirichlet condition. Otherwise, we say that the population will be washed out.

Since the next generation operator Γ has a formula similar to that of the next generation operator defined in [25] (see equation (2.13) therein), applying the results of R_0 analysis in [25] to this paper, we see that if $R_0 > 1$ ($R_0 < 1$), then the number

of adults in the next generation will be more (less) than the current adults. Hence, after many generations, more and more (less and less) adults will be reproduced by their parents. Therefore, we conclude that the population will persist in the river if $R_0 > 1$ but will be washed out if $R_0 < 1$.

For most cases it is impossible to find an analytical expression for R_0. We apply one of the principal projection methods, the collocated method, reviewed in [4, sect. 3.1.1] and restated in [25], to numerically approximate R_0. The details about this numerical method are provided in section S2 in the supplemental material (M105782SupMat.pdf [local/web 265KB]).

3.4. Connections between $R_\delta(x)$ and R_0. Although the next generation operator Γ is not involved in the definitions of $R_\delta(x)$ (3.9), the measures $R_\delta(x)$ and R_0 are actually related to the next generation operator. In fact, $R_\delta(x)$ can alternatively be defined as

$$R_\delta(x) = \int_0^L \Gamma\delta(y-x)dy; \tag{3.14}$$

here $\delta(\cdot)$ is the Dirac delta distribution. In fact, if an adult individual is introduced at location x, then the adult stage has an initial distribution

$$A(y) = \delta(y-x),$$

where $y \in [0, L]$ and x is fixed. By (3.10), the next generation population will be distributed according to

$$\begin{aligned}(\Gamma A)(y) = \Gamma\delta(y-x) &= s_l(y)s_j(y)\int_0^L \frac{r(z)}{1-s_a(z)}\delta(z-x)k(y,z)dz \\ &= s_l(y)s_j(y)\frac{r(x)}{1-s_a(x)}k(y,x).\end{aligned}$$

Integrating over all spatial locations y, we obtain

$$\int_0^L \Gamma\delta(y-x)dy = \frac{r(x)}{1-s_a(x)}\int_0^L s_l(y)s_j(y)k(y,x)dy,$$

which is equivalent to (3.9).

4. Critical domain size. In this section, we find the critical domain size (i.e., the minimum length of suitable river habitat for a population to persist) by analyzing the net generation operator. We consider the special case of model (2.1) where $q, D, m, \sigma, h, r, s_l, s_j$, and s_a are constants and $\varphi(x, n) = 1$. We set the advection rate $Q/q = v$.

Recall that R_0 is the dominant eigenvalue of the next generation operator defined by (3.10); therefore, we solve the eigenvalue problem

$$\Gamma A(x) = \lambda A(x) = \frac{s_l s_j r}{1-s_a}\int_0^L A(y)k(x,y)dy. \tag{4.1}$$

We only consider the special case when $\epsilon = 0$; thus, (4.1) is equivalent to

$$\frac{s_l s_j r h\sigma}{1-s_a}\int_0^L A(y)\hat{k}(x,y)dy = \lambda A(x). \tag{4.2}$$

Applying the linear operator $\mathcal{L}-(m+\sigma)$ to (4.2), we obtain a Sturm–Liouville problem. Then by choosing the threshold value $R_0 = \lambda = 1$ and finding the minimum positive solution of the Sturm–Liouville problem, we find that

$$v < 2\sqrt{D\left(\frac{s_l s_j r\sigma}{(1-s_a)\lambda} - m - \sigma\right)} = 2\sqrt{D\left(\frac{s_l s_j r\sigma}{1-s_a} - m - \sigma\right)} := v^* \tag{4.3}$$

is a necessary condition for the population to persist. When $v < v^*$, the critical domain size, denoted by L_{crit}, under hostile boundary conditions (2.3) is given by

$$L_{\text{crit}}^{\text{hos}} = \frac{2D}{\sqrt{4D\left(\frac{s_l s_j r\sigma}{1-s_a} - m - \sigma\right) - v^2}}\left(\pi - \arctan\sqrt{\frac{4D}{v^2}\left(\frac{s_l s_j r\sigma}{1-s_a} - m - \sigma\right) - 1}\right). \tag{4.4}$$

A full calculation is provided in Appendix C. Since (C.5) in Appendix C implies that $d\lambda/dL > 0$, it follows that $R_0 > 1$ if $L > L_{\text{crit}}^{\text{hos}}$, and $R_0 < 1$ if $L < L_{\text{crit}}^{\text{hos}}$. That is, when the length of the river is longer than the critical domain size, the population can persist in the river; otherwise, the population will be washed out.

Similar calculations show when $v < v^*/\sqrt{2}$, the critical domain size under Danckwerts' boundary conditions is given by

$$L_{\text{crit}}^{\text{Dan}} = \frac{2D}{\sqrt{4D\left(\frac{s_l s_j r\sigma}{1-s_a} - m - \sigma\right) - v^2}} \arctan\frac{\sqrt{\frac{4D}{v^2}\left(\frac{s_l s_j r\sigma}{1-s_a} - m - \sigma\right) - 1}}{\frac{2D}{v^2}\left(\frac{s_l s_j r\sigma}{1-s_a} - m - \sigma\right) - 1}. \tag{4.5}$$

When $v^*/\sqrt{2} < v < v^*$, the critical domain size is

$$L_{\text{crit}}^{\text{Dan}} = \frac{2D}{\sqrt{4D\left(\frac{s_l s_j r\sigma}{1-s_a} - m - \sigma\right) - v^2}}\left(\pi - \arctan\frac{\sqrt{\frac{4D}{v^2}\left(\frac{s_l s_j r\sigma}{1-s_a} - m - \sigma\right) - 1}}{1 - \frac{2D}{v^2}\left(\frac{s_l s_j r\sigma}{1-s_a} - m - \sigma\right)}\right). \tag{4.6}$$

From (4.4)–(4.6), we see that the critical domain sizes increase as advection increases. This is consistent with the intuition that with faster advection, a population will require a larger domain size to persist. The critical domain sizes approach infinity as $v \to v^*$.

The critical domain size under hostile boundary conditions for a single-compartment (unstructured) population in a river was calculated by Speirs and Gurney [31] and then was adjusted by Mckenzie et al. (see equation (3.10) in [25]). If we replace the expression $s_l s_j r\sigma/(1-s_a) - m - \sigma$ in (4.4) with the intrinsic growth rate in [25] (denoted by $r = f - v$), then (4.4) is equivalent to equation (3.10) in [25].

5. Spread in an unbounded domain. In the previous section, we derived conditions for population persistence on a bounded domain. Here, we consider population spread in an unbounded, previously uninhabited domain. We first construct a redistribution kernel based on the dynamics of larval dispersal and settlement. This allows us to convert the original continuous-discrete model (2.1) into stage-structured integrodifference equations. Based on the integrodifference equation model, we calculate the population's asymptotic invasion speeds in the direction of the drift and against the drift.

5.1. Redistribution kernel in an unbounded domain. We construct a redistribution kernel, denoted by $K(x, y)$, in an unbounded domain in this subsection. $K(x, y)$ describes the probability that a larva, released at location y, will settle at location x, where $x, y \in (-\infty, \infty)$. We let $y = 0$ and denote $K(x, 0)$ by $K(x)$ for convenience. We assume that D, v, m, σ, and h are constants and consider

$$\begin{aligned} &u_t = Du_{xx} - vu_x - (m+\sigma)u, \qquad x \in (-\infty, \infty), \quad t \in (0, \tau), \\ &w_t = h\sigma u, \end{aligned} \tag{5.1}$$

subject to the initial conditions

$$u(x, 0) = \delta(x)/h, \quad w(x, 0) = 0. \tag{5.2}$$

Let $K(x) = w(x, \tau)$. Integrating the second equation of (5.1) on $[0, \tau]$, we have $K(x) = h\sigma \int_0^\tau u(x, t)dt$. Thus, integrating the first equation of (5.1) on $[0, \tau]$, we find that $K(x)$ satisfies

$$DK''(x) - vK'(x) - (m+\sigma)K(x) = u(x, \tau) - \delta(x)/h. \tag{5.3}$$

Similar to Theorem 3.1, for simplicity, instead of using (5.3) to compute the kernel $K(x)$, we consider an approximation of (5.3), that is,

$$DK''(x) - vK'(x) - (m+\sigma)K(x) = -\delta(x)/h, \tag{5.4}$$

with an error of solution that is uniformly bounded by $[\exp(-\tau \min_{x\in[0,L]}\{m(x) + \sigma(x)\})] \cdot [\max_{x\in[0,L]}\{h(x)\}]$.

Following steps similar to those in section 4.2 of [23], we are able to derive an explicit expression for $K(x)$, which is given by

$$K(x) = \begin{cases} \alpha \exp\{\gamma_1 x\}, & x \le 0, \\ \alpha \exp\{\gamma_2 x\}, & x \ge 0, \end{cases} \tag{5.5}$$

where

$$\alpha = \frac{\sigma}{\sqrt{v^2 + 4D(m+\sigma)}}, \quad \gamma_{1,2} = \frac{v}{2D} \pm \sqrt{\Big(\frac{v}{2D}\Big)^2 + \frac{m+\sigma}{D}}.$$

One can obtain an expression for $K(x, y)$ by replacing 0 by y and x by $x - y$ on the right side of (5.5).

Actually, we are able to find an exact expression for the redistribution kernel $K(x)$ by explicitly solving (5.1)–(5.2) (see Appendix D for details). Noticing that the exact expression of $K(x)$ ((D.3) in Appendix D) is given by an integral with respect to t, we will use (5.5), instead of (D.3), to calculate spreading speeds in the next subsection.

5.2. Spreading speed. From the definition of the redistribution kernel $K(x, y)$, we see that in an unbounded domain, at the end of the dispersal stage, the settled larvae, reproduced by the adults with density $A(x, n)$, will be distributed according to

$$w(x, \tau) = \int_{-\infty}^{\infty} r(y)A(y, n)K(x, y)dy, \quad -\infty < x < \infty. \tag{5.6}$$

Substituting (5.6) into the third equation of (2.1), we obtain the following stage-structured integrodifference equation model:

$$\begin{aligned} &J(x, n+1) = \varphi(x, n)s_l(x) \textstyle\int_{-\infty}^{\infty} r(y)A(y, n)K(x, y)dy, \quad -\infty < x < \infty, \\ &A(x, n+1) = \varphi(x, n)[s_j(x)J(x, n) + s_a(x)A(x, n)], \quad -\infty < x < \infty. \end{aligned} \tag{5.7}$$

The main purpose of this subsection is to calculate the upstream and downstream population spreading speeds based on model (5.7). We assume that the environment is spatially homogeneous. This implies that the vital rates depend only on local population density and not explicitly on spatial location, and that the redistribution kernel depends only on relative distance $x - y$. With this assumption, let $(J(x,n), A(x,n))^T = \mathbf{N}(x,n)$; then according to the linear conjecture, the rate of spread of the population modeled by (5.7) is governed by its linearization near $(0,0)$,

$$\mathbf{N}(x,n+1) = \int_{-\infty}^{\infty} [\mathbf{B} \circ \mathbf{K}(x-y)]\mathbf{N}(y,n)dy, \tag{5.8}$$

where $\mathbf{B}$ is the projection matrix given by

$$\mathbf{B} = \begin{pmatrix} 0 & s_l r \\ s_j & s_a \end{pmatrix}, \tag{5.9}$$

$\mathbf{K}(x-y)$ is the dispersal matrix given by

$$\mathbf{K}(x-y) = \begin{pmatrix} \delta(x-y) & K(x-y) \\ \delta(x-y) & \delta(x-y) \end{pmatrix}, \tag{5.10}$$

and symbol $\circ$ is the Hadamard product indicating element by element multiplication. If there is no dispersal during a given transition, the associated kernel is the Dirac delta function $\delta(x-y)$. That is, individuals stay where they are with probability one.

The spreading speed is the asymptotic velocity with which a locally introduced population eventually spreads spatially into the surrounding habitat. We take the approach of Neubert and Caswell [27], based on the work of Liu [20], and calculate the spreading speeds c_* as the minimum of a dispersion relation that relates traveling wave speed c to wave steepness θ for the traveling wave solution to (5.8). However, we extend this approach to account for the fact that spread in upstream and downstream directions will be at different speeds.

We first consider a fixed profile traveling downstream with some constant speed, c^+. Thus, we assume a traveling wave solution of the form $\mathbf{N}(x,n+1) = \mathbf{N}(x-c^+,n)$. Plugging this into (5.8), we have

$$\mathbf{N}(x-c^+,n) = \int_{-\infty}^{\infty} [\mathbf{B} \circ \mathbf{K}(x-y)]\mathbf{N}(y,n)dy. \tag{5.11}$$

We consider the exponential ansatz

$$\mathbf{N}(x,n) = \mathbf{\Psi} e^{-\theta x}, \tag{5.12}$$

where $\theta > 0$ and $\mathbf{\Psi}$ is a vector that represents the population densities of the two stages at point $x = 0$ in year n.

Substituting (5.12) into (5.11), we obtain

$$e^{\theta c^+ - \theta x}\mathbf{\Psi} = \left[\mathbf{B} \circ \int_{-\infty}^{\infty} \mathbf{K}(x-y)e^{-\theta y}dy\right]\mathbf{\Psi}. \tag{5.13}$$

Changing variables to $\xi = x - y$ and x yields

$$e^{\theta c^+}\mathbf{\Psi} = \left[\mathbf{B} \circ \int_{-\infty}^{\infty} \mathbf{K}(\xi)e^{\theta \xi}d\xi\right]\mathbf{\Psi}, \tag{5.14}$$

where the matrix

$$\mathbf{B} \circ \int_{-\infty}^{\infty} \mathbf{K}(\xi) e^{\theta\xi} d\xi = \begin{pmatrix} 0 & s_l r M(\theta) \\ s_j & s_a \end{pmatrix} := \mathbf{H}(\theta),$$

with $M(\theta) = \int_{-\infty}^{\infty} K(\xi) e^{\theta\xi} d\xi$, which is referred to as the moment-generating function of the redistribution kernel $K(\xi)$. Using the expression for $K(\xi)$ (see (5.5)), we find that when $\gamma_2 + \theta < 0$ (i.e., $\theta < -\gamma_2 = \sqrt{(v/2D)^2 + (m+\sigma)/D} - v/(2D)$), the moment-generating function $M(\theta)$ exists and is given by

$$M(\theta) = \alpha \left[\int_{-\infty}^{0} e^{(\gamma_1+\theta)\xi} d\xi + \int_{0}^{\infty} e^{(\gamma_2+\theta)\xi} d\xi \right] = \alpha \left(\frac{1}{\gamma_1 + \theta} - \frac{1}{\gamma_2 + \theta} \right).$$

(Note that $\gamma_1 + \theta$ is always positive.)

Therefore, if $\theta < -\gamma_2$, then applying the results from [27], we find that the downstream traveling wave speed is given by

$$c^+(\theta) = \frac{1}{\theta} \ln \rho[\mathbf{H}(\theta)] = \frac{1}{\theta} \ln \frac{s_a + \sqrt{s_a^2 + 4 s_l s_j r M(\theta)}}{2}, \tag{5.15}$$

and thus the (asymptotic) downstream spreading speed is given by

$$c_*^+ = \inf_{0<\theta<-\gamma_2} \frac{1}{\theta} \ln \rho[\mathbf{H}(\theta)] = \inf_{0<\theta<-\gamma_2} \frac{1}{\theta} \ln \frac{s_a + \sqrt{s_a^2 + 4 s_l s_j r M(\theta)}}{2}, \tag{5.16}$$

where $\rho[\cdot]$ denotes the dominate eigenvalue of the matrix $\mathbf{H}(\theta)$. We observe that $c^+(\theta)$ approaches infinity as $\theta \to 0^+$ and $\theta \to (-\gamma_2)^-$. Thus, $c^+(\theta)$ attains a minimum on $(0, -\gamma_2)$. Setting the derivative of the function $c^+(\theta)$ to zero, we get a critical point θ_*^+ such that $c_*^+ = \frac{1}{\theta_*^+} \ln \rho[\mathbf{H}(\theta_*^+)]$.

For the upstream traveling wave speed c^-, we consider the corresponding ansatz $\mathbf{N}(x, n) = \mathbf{\Psi} e^{\theta x}$, where $\theta > 0$. Accordingly, if $\theta < \gamma_1$, then the upstream traveling wave speed is given by

$$c^-(\theta) = \frac{1}{\theta} \ln \rho[\mathbf{H}(-\theta)] = \frac{1}{\theta} \ln \frac{s_a + \sqrt{s_a^2 + 4 s_l s_j r M(-\theta)}}{2}, \tag{5.17}$$

and the (asymptotic) upstream spreading speed is given by

$$c_*^- = \inf_{0<\theta<\gamma_1} \frac{1}{\theta} \ln \rho[\mathbf{H}(-\theta)] = \inf_{0<\theta<\gamma_1} \frac{1}{\theta} \ln \frac{s_a + \sqrt{s_a^2 + 4 s_l s_j r M(-\theta)}}{2}. \tag{5.18}$$

Note that $M(-\theta)$ exists when $\theta < \gamma_1$. Also, we are able to get a critical point θ_*^- such that $c_*^- = \frac{1}{\theta_*^-} \ln \rho[\mathbf{H}(\theta_*^-)]$.

In Appendix E, we provide an alternative way to calculate the spreading speeds c_*^+ and c_*^-, in which one does not have to take the infimum as in (5.16) or (5.18).

It is worth pointing out that in section 5.1, for simplicity we obtained the expression of redistribution kernel $K(x)$ (5.5) by letting $u(x, \tau) = 0$. Actually, $u(x, \tau)$, which represents the larval density in the drift at the end of breeding season, is extremely small, so (5.5) is a good approximation to the exact expression of $K(x)$ ((D.3) in Appendix D), and we expect that the spreading speeds we obtain in this section are good approximations to the exact spreading speeds. However, if we use the exact expression of $K(x)$, then it would be very difficult to show the existence of the moment-generating functions; hence we are unable to obtain the analytical expressions for spreading speeds.

6. Model parameterization. We estimate the parameters for model (2.1)–(2.2) by connecting model to experimental data in the literature (see section S3 in the supplemental material (M105782SupMat.pdf [local/web 265KB]) for details). In particular, we consider the dependence of population survival rates and the growth of shell length on temperature. The results of model parameterization are then used to investigate how the temperature and water flow affect the long-term dynamics of zebra mussels in a river. Population survival rates are related to temperature T by the quadratic logistic regression (the estimated results for model parameters τ, m, σ, r, and D are listed in Table 6.1)

$$s_l(T) = s_j(T) = s_a(T) = \frac{\exp(b_0 + b_1 T + b_2 T^2)}{1 + \exp(b_0 + b_1 T + b_2 T^2)}, \tag{6.1}$$

plus our simplifying assumption that $s_l(T) = s_j(T) = s_a(T)$. We ignore the effect of temperature on larval length and choose $\ell_l(T) = 2$ mm. We estimate that the average juvenile shell length is related to temperature T by

$$\ell_j(T) = \frac{24.71 \exp(-8.89 + 0.66T - 0.02T^2)}{1 + \exp(-8.89 + 0.66T - 0.02T^2)}, \tag{6.2}$$

and the average adult shell length is related to temperature T by

$$\ell_a(T) = \frac{31.92 \exp(-7.71 + 0.53T - 0.016T^2)}{1 + \exp(-7.71 + 0.53T - 0.016T^2)}. \tag{6.3}$$

TABLE 6.1
Some of the parameters in the model (2.1)–(2.2).

Symbols	Definitions	Estimated values
τ	longest dispersing time before settling	30 days
m	mortality rate of dispersing larvae	1.44/day
σ	settling rate of dispersing larvae	0.00144/day
r	reproduction rate of adults	4218/year
D	diffusion coefficient	0.4 m^2/second

7. Numerical results. In the previous section, we estimated all parameters, except the flow rate v, the water depth h, and the competition coefficient β, in the model (2.1)–(2.2). In this section, we use the results of model parameterization in section 6 to study how the river flow, temperature, and boundary conditions affect the population persistence through numerical simulations. To do so, we first rescale the model (2.1)–(2.2) into a new system. By doing so, we avoid having to estimate the parameter β, for which data are lacking. We rescale model (2.1)–(2.2) by setting

$$\tilde{u} = \beta \ell_a u, \quad \tilde{w} = \beta \ell_l w, \quad \tilde{J} = \beta \ell_j J, \quad \tilde{A} = \beta \ell_a A.$$

We drop the tildes for convenience and assume that D, q, m, σ, h are constants, so that model (2.1)–(2.2) becomes

$$
\begin{aligned}
&u_t = u_{xx} - vu_x - mu - \sigma u, \quad x \in (0, L), \quad t \in (0, \tau)\\
&w_t = h\sigma u \ell_l/\ell_a, \quad x \in (0, L), \quad t \in (0, \tau),\\
&J(x, n+1) = \psi(x, n) s_l(x, T) w(x, \tau) \ell_j/\ell_l, \quad x \in (0, L),\\
&A(x, n+1) = \psi(x, n)[s_j(x, T) J(x, n) \ell_a/\ell_j + s_a(x, T) A(x, n)], \quad x \in (0, L),\\
&\alpha_1 u(0, t) - \alpha_2 u_x(0, t) = 0, \quad \alpha_3 u(L, t) + \alpha_4 u_x(L, t) = 0, \quad t \in (0, \tau),\\
&u(x, 0) = rA(x, n)/h, \quad w(x, 0) = 0, \quad x \in (0, L),\\
&J(x, 0) = J^0(x), \quad A(x, 0) = A^0(x), \quad x \in (0, L),
\end{aligned}
\tag{7.1}
$$

where

$$
\psi(x, n) = \frac{1}{1 + w(x, \tau) + J(x, n) + A(x, n)}. \tag{7.2}
$$

Note that in the rescaled model (7.1)–(7.2), u has unit 1/area, and v, J, and A are nondimensional. Clearly, system (7.1)–(7.2) has the same long-term dynamics as the original model (2.1)–(2.2). Thus, in what follows, we make numerical simulations based on system (7.1)–(7.2) instead of model (2.1)–(2.2).

7.1. Model solutions, persistence, and washout. First we numerically solve the population model (7.1)–(7.2) by choosing the same temperature $T = 15°\mathrm{C}$ (the population survival rates can be calculated according to (6.1), and the shell lengths can be calculated according to (6.2) and (6.3)) but two different flow velocities (top row of Figure 7.1). We assume that the population is initially introduced in the middle part of the river. The population distributions for the two cases at different time points are shown in the top row of Figure 1. To show the action of the next generation operator, we also numerically approximate R_0 and its eigenfunction $\phi(x)$ (bottom row of Figure 7.1) using the collocation method presented in section S2 in the supplemental material (M105782SupMat.pdf [local/web 265KB]). Figure 7.1 indicates that the net reproductive rate R_0 determines the eventual fate of the population: persistence ($R_0 > 1$) or washout ($R_0 < 1$).

7.2. The effect of water flow on source-sink dynamics. Next we consider the source-sink regions in the river by computing $R_\delta(x)$. The results are presented in Figure 7.2 for two different flow velocities. We compare $R_\delta(x)$ for the population described by (7.1)–(7.2) subject to hostile boundary conditions (left column of Figure 7.2) and Danckwerts' boundary conditions (right column of Figure 7.2). The dispersal described by the Green's function $k(x, 0.5)$ is also shown for low and high flows (bottom row of Figure 7.2). Comparing the solid and dashed lines for each type of boundary condition in Figure 7.2, we see that different flow velocities result in different source-sink regions and different dispersal kernels. More precisely, $R_\delta(x)$ decreases with increasing flow velocity, which leads to decreased source regions (where $R_\delta(x) > 1$) and increased sink regions (where $R_\delta(x) < 1$). Moreover, increased flow velocity leads to decreased dispersal in the upstream direction but increased dispersal in the downstream direction. This indicates that larvae are easily washed downstream but hardly disperse upstream as the flow velocity increases.

Recall that under hostile boundary conditions, the larvae disappear from the river patch once they reach the downstream boundary, while under Danckwerts' boundary

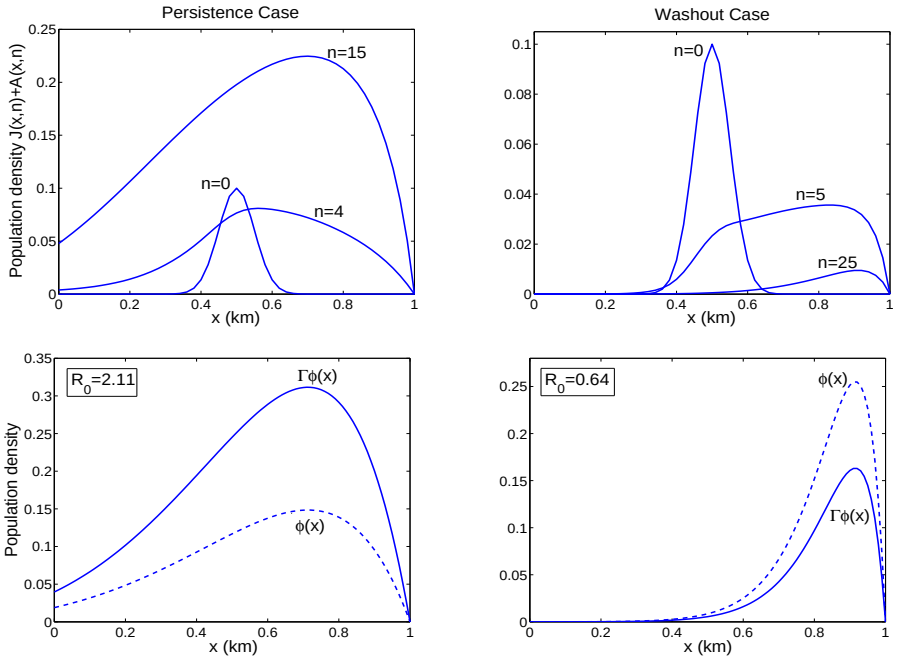

FIG. 7.1. *Top row: Numerical solutions of the population model* (7.1)–(7.2). *Bottom row: The long-term persistence is determined by the action of the next generation operator* Γ *on the dominant eigenfunction* ϕ. *The parameters:* $L = 1$ *km,* $h = 2$ *m,* $T = 15°C$. *Depending on the flow velocity, the population either persists (left column: low flow) or is washed out (right column: high flow) over time.*

conditions, larvae leave the river patch at the same rate as the advection takes them. This is shown by the first row of Figure 7.2. When the flow is low, the source-sink regions are very similar under different boundary conditions. However, when the flow velocity is high, the values of $R_\delta(x)$ differ significantly under different boundary conditions, especially in the downstream regions. Sink regions under hostile boundary conditions may be source regions under Danckwerts' boundary conditions. This is because larvae are washed downstream more quickly with increasing flow; hence the downstream conditions play a more important role in determining whether larvae are able to settle down and produce enough offspring to the next generation.

7.3. The effect of interaction between temperature and river flow on R_δ and R_0. According to the life cycle of zebra mussels, our population model (2.1) assumes that river flow affects the larvae dispersal in the drift, and water temperature affects the survival and growth of settled larvae, juveniles, and adults on the benthos. To understand how the river flow and water temperature interact to influence the source-sink regions and R_0, we consider the average of $R_\delta(x)$, which can be calculated by $\int_0^L R_\delta(x)dx/L := \overline{R_\delta(x)}$, as a function of flow velocity (v) and temperature (T), and we plot the contour line on which $\overline{R_\delta(x)} = 1$ (thin lines in Figure 7.3). For the same range of v and T, we also calculate R_0 and plot the contour lines on which $R_0 = 1$ (thick lines in Figure 7.3). Again, we consider two different boundary conditions: hostile boundary conditions (left panel of Figure 7.3) and Danckwerts' boundary conditions (right panel of Figure 7.3). As shown by Figure 7.3, the maximum flow speed permitting that $\overline{R_\delta(x)} > 1$ ($R_0 > 1$) under hostile boundary

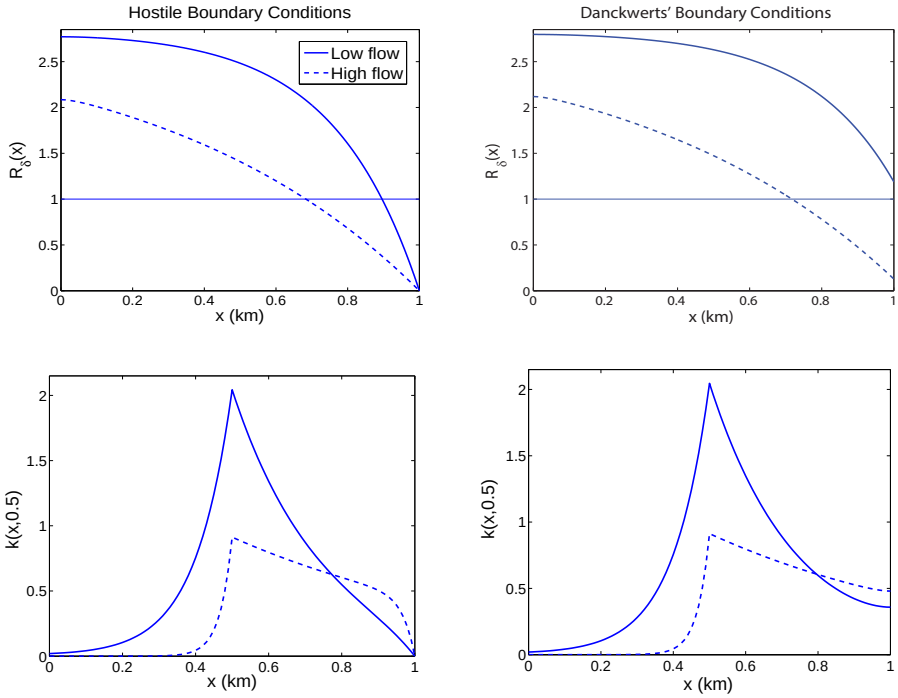

FIG. 7.2. *Source-sink regions described by $R_\delta(x)$ (top row) and corresponding dispersal kernels $k(x, 0.5)$ (bottom row) for different flow velocities and different boundary conditions. Left column: Hostile boundary conditions. Right column: Danckwerts' boundary conditions. The parameters: $L = 1$ km, $h = 2$ m, $T = 15°C$.*

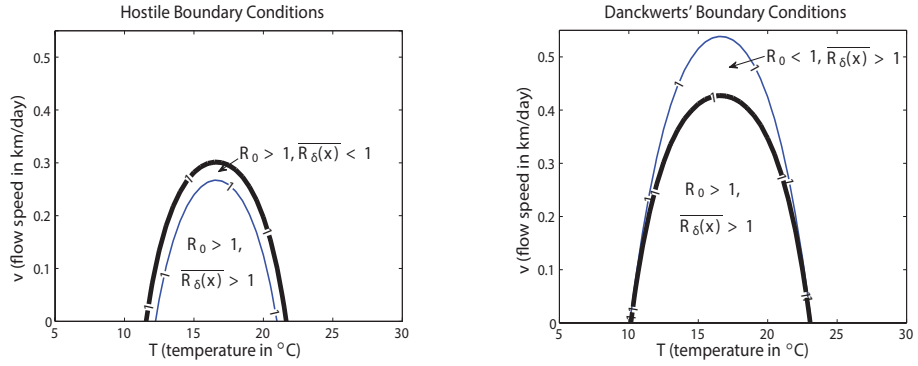

FIG. 7.3. *The average of $R_\delta(x)$ for the entire river and R_0 for a range of flow speeds and water temperatures under hostile boundary conditions (left panel) and Danckwerts' boundary conditions (right panel). Thin contour lines: $\overline{R_\delta(x)} = 1$. Thick contour lines: $R_0 = 1$. The parameters: $L = 0.5$ km, $h = 2$ m.*

conditions is lower than the maximum flow speed permitting that $\overline{R_\delta(x)} > 1$ ($R_0 > 1$) under Danckwerts' boundary conditions.

As we mentioned earlier, as a measure of population persistence, $R_\delta(x)$ does not inform us about the global persistence or extinction. From Figure 7.3, we see that it is possible to have $R_0 > 1$ even when $\overline{R_\delta(x)} < 1$ (left panel of Figure 7.3). It is also

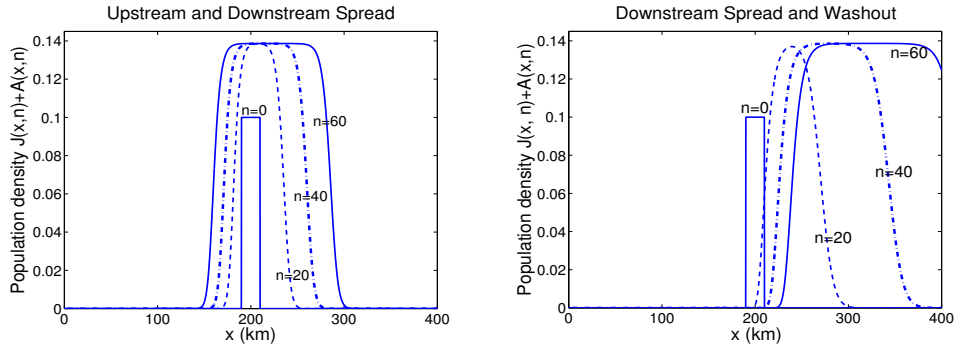

FIG. 7.4. *The total density of juveniles and adults in different years n. Left panel: The flow velocity is low, and the population spreads both upstream and downstream. Right panel: The flow velocity is high, and the population spreads only downstream and is washed out. The parameters:* $L = 400$ *km,* $h = 2$ *m,* $T = 10°C$.

possible to have $R_0 < 1$ even when $\overline{R_\delta(x)} > 1$ (right panel of Figure 7.3). In other words, the population might or might not be able to successfully invade even if the majority of the domain is a source. Therefore, the mean values of $R_\delta(x)$ cannot be used to determine the global persistence or extirpation of the population in a river.

We also choose a large river length L to make the same numerical simulations; the two different boundary conditions yield similar results. This indicates that boundary conditions play a less important role if the river length becomes larger.

7.4. The effect of flow on the population spread. To illustrate the effect of flow velocity on the population spread in a river, we show two possible outcomes in Figure 7.4. When the flow velocity is low, the population spreads in both directions with a bias downstream (left panel of Figure 7.4). When flow velocity is high, the population spreads only downstream and is washed out eventually.

7.5. Connection between the upstream spreading speed and the critical domain size. If a population cannot spread upstream but is washed downstream, it will not persist. Hence, persistence and ability of upstream propagation should be closely connected. Figure 7.5 shows the dependence of the upstream spreading speed (c_*^-), the critical domain size for hostile boundary condition ($L_{\text{crit}}^{\text{hos}}$), and the critical domain size for Danckwerts' boundary conditions ($L_{\text{crit}}^{\text{Dan}}$) on the flow velocity v. We see from Figure 7.5 that the critical domain sizes are increasing functions of v, and that at the threshold value $v = v^* \approx 1.81$ km/day (see (4.3) for the expression of v^*), the critical domain sizes become infinity. On the other hand, as v increases from zero to v^*, the upstream spreading speed c_*^- decreases until it reaches zero. That is, the threshold flow velocity that allows the population to persist on a finite domain is the same as the upper limit of flow rate that allows the population to spread upstream.

8. Discussion. While some species spread upstream in river environments, not all invasive species are successful in spreading upriver. Here the dynamics of unidirectional water flow in rivers play a role in determining invasion success. In this paper, we develop a hybrid continuous/discrete-time model to describe the dynamics of invasive freshwater mussels in rivers. In the model, a reaction-advection-diffusion equation coupled to an ordinary differential equation describes the larval dispersal in the drift and settling to the benthos, while two difference equations describe the population growth on the benthos. We applied the spatial model to understand the

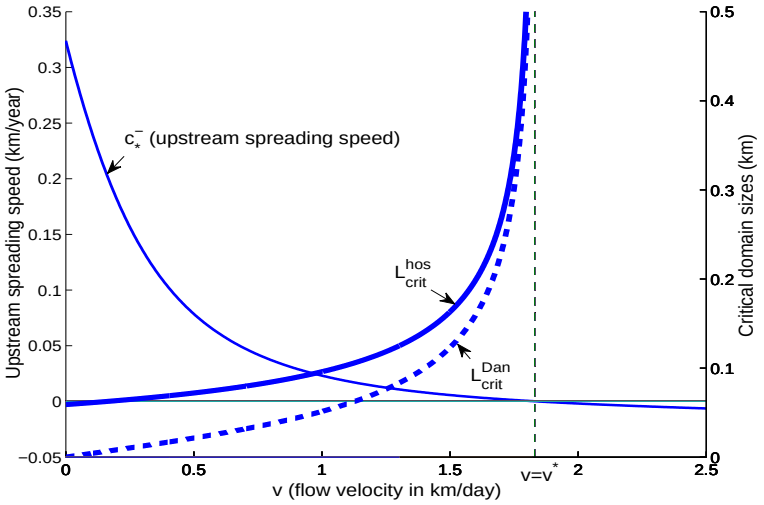

FIG. 7.5. *The dependence of critical domain size for hostile boundary conditions (thick solid curve), critical domain size for Danckwerts' boundary conditions (dashed curve), and the upstream spreading speed (thin solid curve) on flow velocity v. The parameters: $T = 10°C$; other parameters, except v, are the same as those in Figure* 7.1.

interaction between population growth and dispersal, water temperature, and river flow in determining upstream invasion success of zebra mussels. Theoretically, we extended the three measures of population persistence, $R_{\text{loc}}(x)$, $R_\delta(x)$, and R_0, which were defined for a single-compartment model in [25], to our hybrid stage-structured model. These measures are related in the context of a next generation operator. We then found the critical domain size for the population to persist in a river by analyzing the next generation operator. According to the advection-diffusion-reaction equation in the model that governs the larval dispersal, we derived a dispersal kernel in an unbounded domain. Such a kernel allows us to consider a related model of integrodifference equations. We calculated the upstream and downstream spreading speeds of the population based on the integrodifference equation model. The spatial model was parameterized based on experimental data in the literature. In terms of the results of model parameterization, we analyzed the model numerically to determine conditions for persistence as a function of temperature and flow rate.

When we connected the model to experimental data via model parameterization, we assumed that settled larvae, juveniles, and adults have the same survival rates, because data are lacking. In practice, different stages of zebra mussels may have different sensitivities to temperature; therefore, more data are needed to yield more precise quantitative results. Furthermore, as we mentioned in the introduction, many other environmental variables such as turbidity, calcium concentration, and food source also affect the population survival and growth. Thus it may be appropriate to study how the other environmental factors affect the population persistence in a river if data are available.

Deep pools and shallows in a river are examples of heterogeneities that typically occur on shorter spatial scales than the whole stretch of a river. It would be interesting to further investigate how the heterogeneous landscapes affect the successful invasion of zebra mussels. We expect that river heterogeneity may yield a situation where zebra mussels can persist in rivers even when they cannot spread upstream.

In addition, it might be worth studying how the critical domain size for an invasive species (zebra mussel) depends on the river heterogeneity. This would extend the theory of critical domain size in [21]. In that paper, based on a single-compartment model, the authors analyzed the minimum length that supports a population by considering a spatially periodic pool-shallow river. Furthermore, the living conditions for an invasive species and the hydrodynamics environment in a river can vary seasonally. The theory developed here could be extended to more general models by including seasonal variations in population growth [13, 12] and temporal variations of flow rate [11].

The spatial model (2.1) can also be used to describe the dynamics of other related invasive species, such as quagga mussel (*Dreissena bugensis*) in rivers. Quagga and zebra mussels possess similar morphologies, life cycles, and functional ecologies. In different types of water bodies, zebra and quagga mussels either coexist or one species excludes the other (reviewed by [15] and [29]). These cases suggest that patterns of relative dominance and competitive exclusion among these species may vary over space and time, presumably under the influence of environmental variables. A competition model given by a system of integrodifference equations has been developed to explain interactions of zebra and quagga mussel in lakes [17], but the unidirectional flow conditions of rivers will increase dynamical complexity, which may permit weaker competitors but stronger dispersers to coexist in abundance at upstream locations [22]. As a future effort, we plan to extend our single-species model to a competition model that describes the competing dynamics of zebra and quagga mussels in rivers, assuming that larvae disperse in the drift, and that juveniles and adults compete for resources on the benthos. The model will then be used to understand how the interactions between flow rate and environmental factors impact the persistence, extinction, and competitive exclusion.

Appendix A. Proof of Theorem 3.1. We take the dispersal kernel $k(x, y)$ as the function $w(x, \tau)$, and $w(x, t)$ is the second component of the solution of the system

$$\begin{aligned} u_t &= \mathcal{L}u - m(x)u - \sigma(x)u, \\ w_t &= h(x)\sigma(x)u, \end{aligned} \tag{A.1}$$

subject to the initial conditions

$$u(x, 0) = \delta(x - y)/h(x), \quad w(x, 0) = 0,$$

and the same boundary conditions as (2.1). Thus, integrating the second equation of (A.1), we obtain

$$k(x, y) = w(x, \tau) = h(x)\sigma(x) \int_0^\tau u(x, t)dt := h(x)\sigma(x)\tilde{k}(x, y).$$

For a fixed y, integrating the first equation of (A.1) on $[0, \tau]$, we have

$$u(x, \tau) - \frac{\delta(x - y)}{h(x)} = \int_0^\tau \left[\mathcal{L}u - m(x)u - \sigma(x)u\right] dt. \tag{A.2}$$

Simple calculation gives

$$\begin{aligned}
&\int_0^\tau [\mathcal{L}u - m(x)u - \sigma(x)u]dt \\
&= \frac{1}{q(x)}\frac{d}{dx}\left(D(x)q(x)\frac{d}{dx}\int_0^\tau u(x,t)dt\right) - \frac{Q}{q(x)}\frac{d}{dx}\int_0^\tau u(x,t)dt \\
&\quad - (m(x)+\sigma(x))\int_0^\tau u(x,t)dt \\
&= \mathcal{L}\tilde{k}(x,y) - [m(x)+\sigma(x)]\tilde{k}(x,y).
\end{aligned} \tag{A.3}$$

A combination of (A.2) and (A.3) yields

$$\mathcal{L}\tilde{k}(x,y) - [m(x)+\sigma(x)]\tilde{k}(x,y) = u(x,\tau) - \delta(x-y)/h(x). \tag{A.4}$$

To obtain boundary conditions, we integrate $\alpha_1 u(x,t) - \alpha_2 u_x(x,t)$ on $[0,\tau]$ to get

$$\textstyle\int_0^\tau [\alpha_1 u(x,t) - \alpha_2 u_x(x,t)]dt = \alpha_1\tilde{k}(x,y) - \alpha_2\tilde{k}'(x,y).$$

Letting $x = 0$ and using the first boundary condition in (2.1), we obtain $\alpha_1\tilde{k}(0,y) - \alpha_2\tilde{k}'(0,y) = 0$. Similarly, we can obtain the second boundary condition $\alpha_3\tilde{k}(L,y) + \alpha_4\tilde{k}'(L,y) = 0$.

We assume that $\hat{k}(x,y)$ is a solution of (3.8) and let $\epsilon(x,y) = \tilde{k}(x,y) - \hat{k}(x,y)$. From the first equation of (A.1), we see that $u(x,\tau) \to 0$ as $\tau \to \infty$; hence $\epsilon \to 0$ as $\tau \to \infty$. To estimate ϵ for a finite τ, we define a linear operator with respect to x:

$$\mathcal{M}_x := -h(x)\mathcal{L} + [m(x)+\sigma(x)]h(x).$$

From (A.4), we see that $\tilde{k}(x,y)$ satisfies

$$\mathcal{M}_x\tilde{k}(x,y) = -h(x)u(x,\tau) + \delta(x-y), \tag{A.5}$$

subject to the above-mentioned homogeneous boundary conditions. On the other hand, from (3.8), we see that $\hat{k}(x,y)$ satisfies

$$\mathcal{M}_x\hat{k}(x,y) = \delta(x-y), \tag{A.6}$$

subject to the same boundary conditions.

Subtracting (A.6) from (A.5), we find that $\epsilon(x,y)$ satisfies

$$\mathcal{M}_x\epsilon(x,y) = -h(x)u(x,\tau), \tag{A.7}$$

subject to the same boundary conditions. A combination of (A.6) and (A.7) yields

$$\epsilon(x,y) = \int_0^L h(z)u(z,\tau)\hat{k}(x-z,y)dz. \tag{A.8}$$

For a finite τ, $u(z,\tau)$ is the larval density at location z at the end of breeding season after a larva is reproduced at location x and then experiences dispersal, settlement, and death. If this initially introduced larva does not disperse, then its density at location x is governed by the decay equation

$$\begin{aligned}
&\tilde{u}_t = -m(x)\tilde{u} - \sigma(x)\tilde{u}, \\
&\tilde{u}(x,0) = 1.
\end{aligned} \tag{A.9}$$

Clearly, the solution of this equation satisfies $\tilde{u}(x,t) \le \exp(-t\min_{x\in[0,L]}\{m(x)+\sigma(x)\})$. Thus, with dispersal, we have that $u(z,\tau) \le \exp(-\tau\min_{z\in[0,L]}\{m(z)+\sigma(z)\})$ for any $z \in [0,L]$. Noticing that $\int_0^L \hat{k}(x-z,y)dy \le 1$, we estimate that

$$|\epsilon(x,y)| \le \max_{z\in[0,L]}\{h(z)u(z,\tau)\} \le \max_{z\in[0,L]}\{h(z)\}\exp\Big(-\tau\min_{z\in[0,L]}\{m(z)+\sigma(z)\}\Big). \tag{A.10}$$

Appendix B. Green's function $\hat{k}(x,y)$ in (3.8). If the parameters q, D, m, σ, and h in the first two equations of model (2.1) are constants, then the Green's function in the ordinary boundary value problem (3.8) is given by

$$\hat{k}(x,y) = \begin{cases} C_1(y)e^{\theta_1 x} + C_2(y)e^{\theta_2 x}, & x < y, \\ C_3(y)e^{\theta_1 x} + C_4(y)e^{\theta_2 x}, & x \ge y, \end{cases} \tag{B.1}$$

where $\theta_{1,2} = [v \pm \sqrt{v^2 + 4D(m+\sigma)}]/(2D)$ (the flow velocity Q/q is denoted by v), and $C_1(y), C_2(y), C_3(y)$, and $C_4(y)$ are constants depending on y. For hostile boundary conditions, we have that

$$C_1(y) = \frac{\exp[-(\theta_1+\theta_2)y][\exp(L\theta_2+\theta_1 y) - \exp(L\theta_1+\theta_2 y)](-v+D\theta_2)}{D(\theta_1-\theta_2)[v\exp(L\theta_1) - v\exp(L\theta_2) + D\exp(L\theta_2)\theta_1 - D\exp(L\theta_1)\theta_2]},$$

$$C_2(y) = \frac{\exp[-(\theta_1+\theta_2)y][\exp(L\theta_2+\theta_1 y) - \exp(L\theta_1+\theta_2 y)](v-D\theta_1)}{D(\theta_1-\theta_2)[v\exp(L\theta_1) - v\exp(L\theta_2) + D\exp(L\theta_2)\theta_1 - D\exp(L\theta_1)\theta_2]},$$

$$C_3(y) = \frac{\exp[L\theta_2-(\theta_1+\theta_2)y][v\exp(\theta_1 y) - v\exp(\theta_2 y) + D\exp(\theta_2 y)\theta_1 - D\exp(\theta_1 y)\theta_2]}{D(-\theta_1+\theta_2)[v\exp(L\theta_1) - v\exp(L\theta_2) + D\exp(L\theta_2)\theta_1 - D\exp(L\theta_1)\theta_2]},$$

$$C_4(y) = \frac{\exp[L\theta_1-(\theta_1+\theta_2)y][-v\exp(\theta_1 y) + v\exp(\theta_2 y) - D\exp(\theta_2 y)\theta_1 + D\exp(\theta_1 y)\theta_2]}{D(\theta_1-\theta_2)[-v\exp(L\theta_1) + v\exp(L\theta_2) - D\exp(L\theta_2)\theta_1 + D\exp(L\theta_1)\theta_2]}.$$

For Danckwerts' boundary conditions, we have that

$$C_1(y) = \frac{\exp[-(\theta_1+\theta_2)y](v-D\theta_2)[-\exp(L\theta_1+\theta_2 y)\theta_1 + \exp(L\theta_2+\theta_1 y)\theta_2]}{D(\theta_1-\theta_2)[D(\exp(L\theta_1) - \exp(L\theta_2))\theta_1\theta_2 + v(-\exp(L\theta_1)\theta_1 + exp(L\theta_2)\theta_2)]},$$

$$C_2(y) = \frac{\exp[-(\theta_1+\theta_2)y](v-D\theta_1)[\exp(L\theta_1+\theta_2 y)\theta_1 - \exp(L\theta_2+\theta_1 y)\theta_2]}{D(\theta_1-\theta_2)[D(\exp(L\theta_1) - \exp(L\theta_2))\theta_1\theta_2 + v(-\exp(L\theta_1)\theta_1 + \exp(L\theta_2)\theta_2)]},$$

$$C_3(y) = \frac{-\exp[L\theta_2-(\theta_1+\theta_2)y]\theta_2[-v\exp(\theta_1 y) + v\exp(\theta_2 y) - D\exp(\theta_2 y)\theta_1 + D\exp(\theta_1 y)\theta_2]}{D(\theta_1-\theta_2)[D(\exp(L\theta_1) - \exp(L\theta_2))\theta_1\theta_2 + v(-\exp(L\theta_1)\theta_1 + \exp(L\theta_2)\theta_2)]},$$

$$C_4(y) = \frac{-\exp[L\theta_1-(\theta_1+\theta_2)y]\theta_1[v\exp(\theta_1 y) - v\exp(\theta_2 y) + D\exp(\theta_2 y)\theta_1 - D\exp(\theta_1 y)\theta_2]}{D(\theta_1-\theta_2)[D(\exp(L\theta_1) - \exp(L\theta_2))\theta_1\theta_2 + v(-\exp(L\theta_1)\theta_1 + \exp(L\theta_2)\theta_2)]}.$$

Appendix C. Calculation of critical domain size. Applying the linear operator $\mathcal{L} - (m+\sigma)$ to (4.2), we have

$$\frac{s_l s_j r h \sigma}{1-s_a}\int_0^L A(y)[\mathcal{L}\hat{k}(x,y) - (m+\sigma)\hat{k}(x,y)]dy = \lambda[\mathcal{L}A(x) - (m+\sigma)A(x)]. \tag{C.1}$$

Using the first equation of (3.8), we get

$$A''(x) - \frac{v}{D}A'(x) + \left(\frac{s_l s_j r\sigma}{(1-s_a)D\lambda} - \frac{m+\sigma}{D}\right)A(x) = 0, \quad x \in (0,L).$$

When $x = 0$, by (4.2) and the second equation of (3.8), we find

$$\alpha_1 A(0) - \alpha_2 A'(0) = \frac{s_l s_j r h \sigma}{(1-s_a)\lambda} \int_0^L A(y)[\alpha_1 \hat{k}(0,y) - \alpha_2 \hat{k}(0,y)]dy = 0.$$

Similarly, using (4.2) and the third equation of (3.8), we can obtain that $\alpha_3 A(L) + \alpha_4 A'(L) = 0$.

We consider the following Sturm–Liouville problem under the hostile boundary condition:

$$\begin{aligned} &A''(x) - \tfrac{v}{D}A''(x) + \left(\tfrac{s_l s_j r\sigma}{(1-s_a)D\lambda} - \tfrac{m+\sigma}{D}\right) A(x) = 0, \quad x \in (0,L), \\ &vA(0) - DA'(0) = 0, \quad A(L) = 0. \end{aligned} \tag{C.2}$$

The characteristic equation for (C.2) is

$$r^2 - \frac{v}{D}r + \left(\frac{s_l s_j r\sigma}{(1-s_a)D\lambda} - \frac{m+\sigma}{D}\right) = 0,$$

with discriminant

$$\Delta(\lambda) = \left(\frac{v}{D}\right)^2 - 4\left(\frac{s_l s_j r\sigma}{(1-s_a)D\lambda} - \frac{m+\sigma}{D}\right).$$

It is straightforward to show that (C.2) has zero solution only when $\Delta \geq 0$. Thus, positive solutions of (C.2) exist only when $\Delta < 0$ or, equivalently, when

$$v < 2\sqrt{D\left(\frac{s_l s_j r\sigma}{(1-s_a)\lambda} - m - \sigma\right)}. \tag{C.3}$$

Notice that the population persistence in a domain of length L occurs when $\lambda = R_0 \geq 1$. If $\lambda \geq 1$, then $s_l s_j r\sigma/((1-s_a)D\lambda) \leq s_l s_j r\sigma/((1-s_a)D)$, in which case (C.3) implies

$$v < 2\sqrt{D\left(\frac{s_l s_j r\sigma}{(1-s_a)\lambda} - m - \sigma\right)} \leq 2\sqrt{D\left(\frac{s_l s_j r\sigma}{1-s_a} - m - \sigma\right)} := v^*.$$

If $v > v^*$, then either (C.2) has no positive solution or a positive solution exists but $\lambda < 1$, which in either case implies that the zero solution is stable and the critical domain size does not exist. Thus $v < v^*$ is a necessary condition for the population to persist. When $v < v^*$, (C.2) has positive solutions taking the form

$$A(x) = \exp\left(\frac{v}{2D}x\right)\left[c_1 \cos\left(\frac{\sqrt{-\Delta(\lambda)}}{2}x\right) + c_2 \sin\left(\frac{\sqrt{-\Delta(\lambda)}}{2}x\right)\right], \tag{C.4}$$

where the constants c_1 and c_2 are determined by the boundary conditions.

To match the left-hand boundary condition, we now require

$$\frac{c_1}{c_2} = \frac{D}{v}\sqrt{-\Delta(\lambda)},$$

while matching the right-hand condition requires

$$\frac{c_1}{c_2} = -\tan\left(\frac{L}{2}\sqrt{-\Delta(\lambda)}\right).$$

A solution matching both boundary conditions thus requires

$$\tan\left(\frac{L}{2}\sqrt{-\Delta(\lambda)}\right) = -\frac{D}{v}\sqrt{-\Delta(\lambda)}. \tag{C.5}$$

Therefore, if $v < v^*$, then substituting $\lambda = R_0 = 1$ into (C.5), we can obtain the critical domain size $L_{\text{crit}}^{\text{hos}}$ under hostile boundary condition (2.3) as the minimum positive solution of (C.5), which is given by

$$L_{\text{crit}}^{\text{hos}} = \frac{2D}{\sqrt{4D\left(\frac{s_l s_j r\sigma}{1-s_a} - m - \sigma\right) - v^2}}\left(\pi - \arctan\sqrt{\frac{4D}{v^2}\left(\frac{s_l s_j r\sigma}{1-s_a} - m - \sigma\right) - 1}\right).$$

Appendix D. An exact expression for redistribution kernel $K(x)$. We first solve the equation

$$u_t = Du_{xx} - vu_x - (m+\sigma)u, \qquad x \in (-\infty, \infty), \quad t \in (0, \tau), \tag{D.1}$$

subject to the initial condition $u(x,0) = \delta(x-y)/h$. A change of dependent variable to $\hat{u}(x,t) = \exp\{(m+\sigma)t\}u(x,t)$ leads to an equation without the decay term, and a transformation of independent variables to $\bar{t} = t$, $\bar{x} = x - vt$ eliminates the advection term. Hence, the advection-diffusion-decay equation (D.1) can be transformed into a single diffusion equation. The complete transformation is

$$u(x,t) = \exp\left\{\frac{v}{4D}(2x - vt) - (m+\sigma)t\right\}\bar{u}(x,t),$$

where $\bar{u}(x,t)$ satisfies

$$\bar{u}_t = D\bar{u}_{xx}. \tag{D.2}$$

A fundamental solution of (D.2) yields a fundamental solution of (D.1),

$$U(x,t) = \frac{1}{\sqrt{4\pi Dt}}\exp\left\{-\frac{x^2}{4Dt}\right\}\exp\left\{\frac{v}{4D}(2x - vt) - (m+\sigma)t\right\}.$$

Using the initial condition $u(x,0) = \delta(x)/h$, we obtain

$$\begin{aligned} u(x,t) &= \int_{-\infty}^{\infty} U(x-z,t)\frac{\delta(z)}{h}dz \\ &= \frac{1}{h\sqrt{4\pi Dt}}\exp\left\{-\frac{x^2}{4Dt}\right\}\exp\left\{\frac{v}{4D}(2x - vt) - (m+\sigma)t\right\}. \end{aligned}$$

Thus, the redistribution kernel

$$\begin{aligned} K(x) &= h\sigma\int_0^{\tau} u(x,t)dt \\ &= \frac{\sigma}{\sqrt{4\pi D}}\exp\left\{\frac{vx}{2D}\right\}\int_0^{\tau}\frac{1}{\sqrt{t}}\exp\left\{-\frac{x^2}{4Dt} - \left(\frac{v^2}{4D} + m + \sigma\right)t\right\}dt. \end{aligned} \tag{D.3}$$

Appendix E. An alternative way to calculate spreading speeds. From (5.15), we see that

$$e^{\theta c^+} = \frac{s_a + \sqrt{s_a^2 + 4s_l s_j r M(\theta)}}{2}. \tag{E.1}$$

We are interested in monotonic (rather than oscillatory) waves and real (rather than complex) roots θ. Real roots emerges as a double root at the second-order contact that is given by differentiating (E.1) with respect to θ (see Appendix A in [16]):

$$c^+ e^{\theta c^+} = \frac{s_l s_j r M'(\theta)}{\sqrt{s_a^2 + 4 s_l s_j r M(\theta)}}. \tag{E.2}$$

Dividing (E.2) by (E.1), we have

$$c^+ = \frac{2 s_l s_j r M'(\theta)}{s_a \sqrt{s_a^2 + 4 s_l s_j r M(\theta)} + s_a^2 + 4 s_l s_j r M(\theta)}. \tag{E.3}$$

A combination of (E.1) and (E.3) leads to a parametric representation for $\theta \in (0, -\gamma_2)$. This representation will yield a downstream spreading speed c_*^+. Similarly, we can find c_*^- using (5.17).

Acknowledgment. The authors are grateful to the anonymous referees for many insightful comments that helped improve the paper.

REFERENCES

[1] D. L. Arnott and M. J. Vanni, *Nitrogen and phosphorus recycling by the zebra mussel (*Dreissena polymorpha*) in the western basin of Lake Erie*, Can. J. Fish. Aquat. Sci., 53 (1996), pp. 646–659, https://doi.org/10.1139/f95-214.

[2] D. T. E. Bastviken, N. F. Caraco, and J. J. Cole, *Experimental measurements of zebra mussel (*Dreissena polymorpha*) impacts on phytoplankton community composition*, Freshwater Biol., 39 (1998), pp. 375–386, https://doi.org/10.1046/j.1365-2427.1998.00283.x.

[3] A. J. Benson, *Chronological history of zebra and quagga mussels (Dreissenidae) in North America,* 1988-2010, in Quagga and Zebra Mussels: Biology, Impacts, and Control, 2nd ed., T. F. Nalepa and D. W. Schloesser, eds., CRC Press, Boca Raton, FL, 2013, pp. 9–31.

[4] F. Chatelin, *The spectral approximation of linear operators with applications to the computation of eigenelements of differential and integral operators*, SIAM Rev., 23 (1981), pp. 495–522, https://doi.org/10.1137/1023099.

[5] J. M. Cushing and Y. Zhou, *The net reproductive value and stability in matrix population models*, Nat. Resour. Model., 8 (1994), pp. 297–333.

[6] D. W. Garton and W. R. Haag, *Seasonal reproductive cycles and settlement patterns of* Dreissena polymorpha *in western Lake Erie*, in Zebra Mussels: Biology, Impacts, and Control, T. F. Nalepa and D. W. Schloesser, eds., Lewis Publishers, Boca Raton, FL, 1993, pp. 111–128.

[7] R. Guenther and J. Lee, *Partial Differential Equations of Mathematical Physics and Integral Equations*, Dover, New York, 1996.

[8] T. G. Horvath, G. A. Lamberti, D. M. Lodge, and W. L. Perry, *Zebra mussel dispersal in lake-stream systems: Source-sink dynamics?*, J. N. Am. Benthol. Soc., 15 (1996), pp. 564–575, https://doi.org/10.2307/1467807.

[9] Q. Huang, H. Wang, A. Ricciardi, and M. A. Lewis, *Temperature- and turbidity-dependent competitive interactions between invasive freshwater mussels*, Bull. Math. Biol., 78 (2016), pp. 353–380, https://doi.org/10.1007/s11538-016-0146-4.

[10] H. A. Jenner and J. P. M. Janssen-Mommen, *Monitoring and control of* Dreissena polymorpha *and other macrofouling bivalves in The Netherlands*, in Zebra Mussels: Biology, Impacts, and Control, T. F. Nalepa and D. W. Schloesser, eds., Lewis Publishers, Boca Raton, FL, 1993, pp. 537–554.

[11] Y. Jin, F. M. Hilker, P. M. Steffler, and M. A. Lewis, *Seasonal invasion dynamics in a spatially heterogeneous river with fluctuating flows*, Bull. Math. Biol., 76 (2014), pp. 1522–1565, https://doi.org/10.1007/s11538-014-9957-3.

[12] Y. Jin and M. A. Lewis, *Seasonal influences on population spread and persistence in streams: Critical domain size*, SIAM J. Appl. Math., 71 (2011), pp. 1241–1262, https://doi.org/10.1137/100788033.

[13] Y. Jin and M. A. Lewis, *Seasonal influences on population spread and persistence in streams: Spreading speeds*, J. Math. Biol., 65 (2012), pp. 403–439, https://doi.org/10.1007/s00285-011-0465-x.

[14] A. Y. Karatayev, L. E. Burlakova, and D. K. Padilla, *Physical factors that limit the distribution and abundance of* Dreissena polymorpha *(Pall.)*, J. Shellfish Res., 17 (1998), pp. 1219–1235.

[15] A. Y. Karatayev, L. E. Burlakova, and D. K. Padilla, *Zebra versus quagga mussels: A review of their spread, population dynamics, and ecosystem impacts*, Hydrobiologia, 746 (2015), pp. 97–112, https://doi.org/10.1007/s10750-014-1901-x.

[16] M. Kot, M. A. Lewis, and P. van den Driessche, *Dispersal data and the spread of invading organisms*, Ecology, 77 (1996), pp. 2027–2042, https://doi.org/10.2307/2265698.

[17] M. Krkošek and M. A. Lewis, *An R_0 theory for source-sink dynamics with application to* Dreissena *competition*, Theor. Ecol., 3 (2010), pp. 25–43, https://doi.org/10.1007/s12080-009-0051-7.

[18] M. A. Lewis and B. Li, *Spreading speed, traveling waves, and minimal domain size in impulsive reaction-diffusion models*, Bull. Math. Biol., 74 (2012), pp. 2383–2402, https://doi.org/10.1007/s11538-012-9757-6.

[19] C. Li and H. Schneider, *Applications of Perron-Frobenius theory to population dynamics*, J. Math. Biol., 44 (2002), pp. 450–462, https://doi.org/10.1007/s002850100132.

[20] R. Lui, *Existence and stability of travelling wave solutions of a nonlinear integral operator*, J. Math. Biol., 16 (1983), pp. 199–220, https://doi.org/10.1007/BF00276502.

[21] F. Lutscher, M. A. Lewis, and E. McCauley, *Effects of heterogeneity on spread and persistence in rivers*, Bull. Math. Biol., 68 (2006), pp. 2129–2160, https://doi.org/10.1007/s11538-006-9100-1.

[22] F. Lutscher, E. McCauley, and M. A. Lewis, *Spatial patterns and coexistence mechanisms in systems with unidirectional flow*, Theoret. Popul. Biol., 71 (2007), pp. 267–277, https://doi.org/10.1016/j.tpb.2006.11.006.

[23] F. Lutscher, E. Pachepsky, and M. A. Lewis, *The effect of dispersal patterns on stream populations*, SIAM J. Appl. Math., 65 (2005), pp. 1305–1327, https://doi.org/10.1137/S0036139904440400.

[24] G. L. Mackie and R. Claudi, *Monitoring and Control of Macrofouling Mollusks in Fresh Water Systems*, 2nd ed., CRC Press, Boca Raton, FL, 2010.

[25] H. W. Mckenzie, Y. Jin, J. Jacobsen, and M. A. Lewis, *R_0 analysis of a spatiotemporal model for a stream population*, SIAM J. Appl. Dyn. Syst., 11 (2012), pp. 567–596, https://doi.org/10.1137/100802189.

[26] E. L. Mills, J. H. Leach, J. T. Carlton, and C. L. Secor, *Exotic species and the integrity of the Great Lakes*, BioSci., 44 (1994), pp. 666–676, https://doi.org/10.2307/1312510.

[27] M. G. Neubert and H. Caswell, *Demography and dispersal: Calculation and sensitivity analysis of invasion speed for structured populations*, Ecology, 81 (2000), pp. 1613–1628, https://doi.org/10.1890/0012-9658(2000)081[1613:DADCAS]2.0.CO;2.

[28] D. Pimentel, R. Zuniga, and D. Morrison, *Update on the environmental and economic costs associated with alien-invasive species in the United States*, Ecol. Econ., 52 (2005), pp. 273–288, https://doi.org/10.1016/j.ecolecon.2004.10.002.

[29] A. Ricciardi and F. G. Whoriskey, *Exotic species replacement: Shifting dominance of dreissenid mussels in the Soulanges Canal, upper St. Lawrence River, Canada*, J. N. Am. Benthol. Soc., 23 (2004), pp. 507–514, https://doi.org/10.1899/0887-3593(2004)023<0507:ESRSDO>2.0.CO;2.

[30] A. Ricciardi, F. G. Whoriskey, and J. B. Rasmussen, *Impact of the* Dreissena *invasion on native unionid bivalves in the upper St. Lawrence River*, Can. J. Fish. Aquat. Sci., 53 (1996), pp. 1434–1444, https://doi.org/10.1139/f96-068.

[31] D. Speirs and W. Gurney, *Population persistence in rivers and estuaries*, Ecology, 82 (2001), pp. 1219–1237, https://doi.org/10.2307/2679984.

[32] M. Sprung, *The other life: An account of present knowledge of the larval phase of* Dreissena polymorpha, in Zebra Mussels: Biology, Impacts, and Control, T. F. Nalepa and D. W. Schloesser, eds., Lewis Publishers, Boca Raton, FL, 1993, pp. 39–53.

[33] I. Stakgold, *Green's Functions and Boundary Value Problems*, 2nd ed., Wiley, New York, 1998.

[34] J. H. Thorp, J. E. Alexander, Jr., B. L. Bukaveckas, G. A. Cobbs, and K. L. Bresko, *Responses of Ohio River and Lake Erie dreissenid molluscs to changes in temperature and turbidity*, Can. J. Fish. Aquat. Sci., 55 (1998), pp. 220–229, https://doi.org/10.1139/f97-242.

[35] D. S. Wilcove, D. Rothstein, J. Dubow, A. Phillips, and E. Losos, *Quantifying threats to imperiled species in the United States*, BioScience, 48 (1998), pp. 607–615.